BIOLOGY OF REPRODUCTION (2016) **95**(3):51, 1–9
Published online before print 27 July 2016.
DOI 10.1095/biolreprod.116.141739

PiggyBac Transposon-Mediated Mutagenesis in Rats Reveals a Crucial Role of *Bbx* in Growth and Male Fertility[1]

Chieh-Ying Wang,[5] Ming-Chu Tang,[5,6] Wen-Chi Chang,[6] Kenryo Furushima,[3,7] Chuan-Wei Jang,[4,7] Richard R. Behringer,[7] and Chun-Ming Chen[2,5,6]

[5]*Department of Life Sciences and Institute of Genome Sciences, National Yang-Ming University, Taipei, Taiwan*
[6]*Laboratory Animal Center, National Yang-Ming University, Taipei, Taiwan*
[7]*Department of Genetics, University of Texas M.D. Anderson Cancer Center, Houston, Texas*

ABSTRACT

Bobby sox homolog (*Bbx*) is an evolutionally conserved gene, but its biological function remains elusive. Here, we characterized defects of *Bbx* mutant rats that were created by PiggyBac-mediated insertional mutagenesis. Smaller body size and male infertility were the two major phenotypes of homozygous *Bbx* mutants. *Bbx* expression profile analysis showed that *Bbx* was more highly expressed in the testis and pituitary gland than in other organs. Histology and hormonal gene expression analysis of control and *Bbx*-null pituitary glands showed that loss of *Bbx* appeared to be dispensable for pituitary histogenesis and the expression of major hormones. BBX was localized in the nuclei of postmeiotic spermatids and Sertoli cells in wild-type testes, but absent in mutant testes. An increased presence of aberrant multinuclear giant cells and apoptotic cells was observed in mutant seminiferous tubules. TUNEL-positive cells costained with CREM (round spermatid marker), but not PLZF (spermatogonia marker), gammaH2Ax (meiotic spermatocyte marker), or GATA4 (Sertoli cell marker). Finally, there were drastically reduced numbers and motility of epididymal sperm from *Bbx*-null rats. These results suggest that loss of BBX induces apoptosis of postmeiotic spermatids and results in spermiogenesis defects and infertility.

HBP2, HMG box-containing protein 2, pituitary, spermiogenesis, testis

INTRODUCTION

In contrast to the many available lines of genetically engineered mice, a large collection of genetically modified rats as alternative models for the functional study of human disease is currently lacking. To create additional genetically modified rats to model human diseases, transposon-tagged insertion in the rat genome has been developed to achieve mutations via nonbiased mutagenesis [1–3]. Previously, we created and demonstrated hybrid Sleeping Beauty and PiggyBac (PB) transposon-mediated insertional mutagenesis in conjunction with a visible coat color marker (tyrosinase) that can be mobilized in the rat genome in the presence of corresponding transposases using a simple breeding scheme [4]. Rats carrying homozygous mutations are ultimately generated for phenotype-driven studies. Lethality and growth restriction can easily be identified during the phenotypic screen if the transposon-disrupted genes are critical for development.

The impairment of fertility by the mutation of specific genes can be directly measured by the capability of progeny production of a test cross of homozygous mutant rats. Male infertility can be caused by a deficit in male germ cell production. Development of male germ cells, the spermatozoa, takes place in the seminiferous tubular epithelium of the testes. This process of spermatogenesis can be subdivided into three phases: the proliferation phase for self-renewal of spermatogonial stem cells and generation of progenitors; the meiotic phase for reduction of chromosome number in spermatocytes; and the spermiogenesis phase for differentiation of haploid spermatids [5, 6]. During these phases, Sertoli cells line the seminiferous tubules, making contact with male germ cells and supporting their development. In sequential cross-sections of seminiferous tubules, distinct morphologies of developing germ cells occur in a nonrandom manner and are defined as stages that vary across species [7]. For example, there are 14 stages in rats [8], 12 stages in mice [9], and 6 stages in humans [10, 11]. The sequential progression of spermatogenic stages over time is called a cycle, and approximately four cycles are required for the completion of spermatogenesis. Because the duration of the spermatogenic process is about 13 days in rats, 8.6 days in mice, and 16 days in humans [5, 7], the entire spermatogenic process from a given spermatogonial stem cell to the generation of spermatocytes, spermatids, and finally spermatozoa requires about 52 days in rats, 33 days in mice, and 64 days in humans [7]. Spermatozoa are then released from contact with Sertoli cells into the seminiferous tubal lumen, travel through the caput and corpus epididymis, and finally reach and are stored in the caudal epididymis.

Bobby sox homolog (*Bbx*) belongs to the high-mobility group (HMG) superfamily of transcription factors and is an evolutionally conserved gene found in worms, flies, fishes, birds, and mammals [12]. BBX is also known as HMG box-containing protein 2, initially identified by functional complementation of defective replication in yeast cells, suggesting that BBX acts as a positive regulator of G1/S transition [13]. *Bbx* is also expressed in ventricular zone progenitor cells in the mouse

[1]This work was supported by National Health Research Institutes grant NHRI-EX105-10515BI, a grant from the Ministry of Education "Aim for the Top University Plan," and Ministry of Sciences and Technology grants MOST 104-2320-B-010-003 and MOST 104-2320-B-010-025 to C.-M.C., and by National Institutes of Health grant RR22904 to R.R.B.
[2]Correspondence: Chun-Ming Chen, Department of Life Sciences and Institute of Genome Sciences, National Yang-Ming University, Taipei, Taiwan 112. E-mail: cmchen@ym.edu.tw
[3]Current address: DS Pharma Biomedical Co., Ltd., Osaka 564-0053, Japan.
[4]Current address: Department of Genetics, University of North Carolina, Chapel Hill, NC 27599.

Received: 8 May 2016.
First decision: 6 June 2016.
Accepted: 14 July 2016.

eISSN: 1529-7268 http://www.biolreprod.org
ISSN: 0006-3363

TABLE 1. Primers used for splinkerette PCR and genotyping.

Primer	Sequence
SpaA	5′-CGAAGAGTAACCGTTGCTAGGAGAGACCGT GGCTGAATGAGACTGGTGTCGACACTAGTGG-3′
SpbB_EcoRI	5′-AATTCCACTAGTGTCGACACCAGTCTCTAATT TTTTTTTTCAAAAAAA-3′
SpbB_BamHI	5′-GATCCCACTAGTGTCGACACCAGTCTCTAATT TTTTTTTTCAAAAAAA-3′
SpbB_XbaI	5′-CTAGCCACTAGTGTCGACACCAGTCTCTAATT TTTTTTTTCAAAAAAA-3′
Sp0F	5′-CGAAGAGTAACCGTTGCTAGGAGAGACC-3′
BacE	5′-AGTGACACTTACCGCATTGACAAG-3′
Sp1F	5′-GTGGCTGAATGAGACTGGTGTCGAC-3′
BacF	5′-TCCTAAATGCACAGCGACGGATTC-3′
Bbx-F	5′-GCCCCCAGATGTTGTTTCTA-3′
Bbx-R	5′-AGGAAATATCGCGAGTGCAG-3′
PB-3′TR (AS)	5′-CGACGGATTCGCGCTATTTAGA-3′

developing neocortex and hippocampus [12, 14]. *Bbx* is repressed by the transcription factor, nuclear factor one X, which plays a key role during neocortex and hippocampus development. These findings imply that *Bbx* regulates the self-renewal and differentiation of neuronal progenitor cells [14]. A recent study also showed that BBX is expressed and involved in odontoblast differentiation of dental pulp stem cells and progenitors [15]. Although these previous studies addressed the role of BBX in the differentiation of some types of stem cells and progenitors, the biological function of *Bbx* remains largely unknown.

Here, we describe a new PB insertion into intron 2 of the *Bbx* locus, referred to as Bbx^{Tn}. We found that the most prominent phenotypes of $Bbx^{Tn/Tn}$ rats were growth restriction and male sterility. *Bbx* was highly expressed in the testes and pituitary gland. Although the loss of *Bbx* appeared to be dispensable for the expression of many pituitary hormonal genes, $Bbx^{Tn/Tn}$ male rats exhibited impairments in testicular function compared with wild-type rats.

MATERIALS AND METHODS

Rats

Wistar Kyoto (WKY/CrlBltw) rats were purchased from BioLASCO Taiwan. The progeny from WKY/CrlBltw rats bred with seed rats, which were generated by crossing PB transposon (Bhr7)-carrying rats and UBC-PB transposase transgenic rats, were screened by splinkerette PCR (see below) to identify new insertions of Bhr7. We identified a male founder carrying the Bhr7 insertion in intron 2 of the *Bbx* locus on chromosome 11. Subsequently, the $Bbx^{Tn/+}$ founder was bred with WKY/CrlBltw females for generating $Bbx^{Tn/+}$ males and females. $Bbx^{Tn/+}$ males and females were intercrossed and produced $Bbx^{Tn/Tn}$ rats and their littermate controls (wild type and $Bbx^{Tn/+}$). All animal experiments were performed with approval of the Institutional Animal Care and Use Committee at National Yang-Ming University.

Splinkerette PCR

We performed splinkerette PCR to identify the location of transposon insertion in the rat genome. The screening procedure was modified from that of Potter and Luo [16]. The primer sequences used in splinkerette PCR are listed in Table 1. First, *Eco*RI-, *Bam*HI-, or *Xba*I-digested genomic DNA was individually ligated to double-stranded splinkerette adaptors, which were prepared by annealing of the primer, SpaA, with SpbB_EcoRI, SpbB_BamHI, or SpbB_XbaI. The primers, Sp0F and BacE, designed from adaptor and transposon sequences, respectively, were used for the first round of PCR. The products from the first round of PCR were amplified by nested PCR using the primers, Sp1F and BacF.

Genotyping

Genotyping was performed by PCR of genomic DNA from 8-day-old rat toes. The *Bbx* wild-type allele was detected by the primers, Bbx-F and Bbx-R, yielding a 513-bp product. The transposon-inserted allele was detected by the primers, Bbx-F and PB-3′TR (AS), yielding a 300-bp product. The primer sequences used for genotyping are listed in Table 1.

Tissue Processing and Histology

Testes were fixed in modified Davidson fixative solution (30% of 37% solution of formaldehyde, 5% glacial acetic acid, and 15% ethanol, and 50% double-distilled H_2O) at 4°C overnight [17]. Pituitary glands were fixed in 10% buffered formalin at 4°C overnight. Next, tissues were washed with 1× PBS and stored in 70% ethanol. Tissues were processed and embedded as previously described [18, 19]. Embedded tissues were sectioned into 5-μm slices. Slides containing the sections were deparaffinized, rehydrated, and stained with Harris hematoxylin and eosin Y (H&E; Sigma-Aldrich) as previously described [18, 19].

Immunohistochemistry

Detailed immunohistochemical and immunofluorescence procedures were previously described [20–22]. Sections were incubated overnight with primary antibodies against BBX (rabbit IgG, 1:200; Proteintech) and growth hormone (GH; goat IgG, 1:100; Santa Cruz Biotechnology) at 4°C overnight. For immunofluorescence, sections were stained with BBX (rabbit IgG, 1:200; Proteintech), GH (goat IgG, 1:100; Santa Cruz Biotechnology), GATA4 (mouse IgG, 1:100; Santa Cruz Biotechnology), γH2AX (mouse IgG, 1:600; BD Pharmingen), PLZF (rabbit IgG, 1:100; Santa Cruz Biotechnology), or CREM1 (rabbit IgG, 1:50; Santa Cruz Biotechnology) at 4°C overnight. After washing, sections were incubated with secondary antibodies conjugated with Alexa Fluor 488 or Alexa Fluor 568 (1:200; Invitrogen) at room temperature for 1 h. Finally, sections were counterstained with 0.5 ng/ml DAPI (4′,6-diamidino-2-phenylindole) for 3 min followed by mounting with fluorescent mounting medium (DakoCytomation).

TUNEL Assay

TUNEL staining was performed using the FragEL DNA Detection Kit (Calbiochem) followed by staining with primary antibodies against GATA4 (mouse IgG, 1:100; Santa Cruz Biotechnology), PLZF (rabbit IgG, 1:100; Santa Cruz Biotechnology), γH2AX (mouse IgG, 1:600; BD Pharmingen), or CREM1 (rabbit IgG, 1:50; Santa Cruz Biotechnology). Nuclei were counterstained with DAPI.

Real-Time RT-PCR

Total RNA from the testes and pituitary glands of 10-wk-old wild-type, *Tn*/+, and *Tn*/*Tn* rats were extracted by TRIzol reagent (Invitrogen) and reverse transcribed to cDNA using the SuperScript III First-Strand Synthesis System (Invitrogen). Real-time PCR reactions were carried out using a Kapa SYBR Fast qPCR kit (Kapa Biosystems). The primers used for real-time PCR are listed in Table 2.

Western Blotting

Protein lysates were extracted from tissue ground with lysis buffer (50 mM Tris-HCl [pH 7.9], 150 mM NaCl, 0.1% SDS, 1% NP40, 0.5% sodium deoxycholate, protease inhibitor cocktail [Roche Applied Science], and phosphatase inhibitor cocktail [Sigma-Aldrich]). Approximately 30 μg of protein lysate per lane was used for SDS-PAGE and immunoblotting. Membranes were blocked with 5% bovine serum albumin or 5% milk in TBS-T and incubated with primary antibodies against BBX (rabbit IgG, 1:1500; Proteintech) or βactin (mouse IgG, 1:5000; Sigma-Aldrich).

Sperm Analysis

The epididymis was dissected into small pieces in warm 1× PBS and incubated in a 37°C water bath for 30 min to release epididymal content, which was collected for sperm counting, sperm smear, and sperm motility analysis. The content was placed into culture dishes, and sperm movement videos were recorded under a microscope. Total sperm numbers were counted with a hemocytometer. To examine sperm morphology, 20 μl of epididymal content was dropped onto slides for sperm smears. The slides were immersed in fixative

TABLE 2. Primers used for real-time RT-PCR.

Primer[a]	Sequence
Bbx-F	5′-CTCTTGGAACGCCAGAGG-3′
Bbx-R	5′-TCTGACGCAACTCAGGTGAC-3′
Prop1-F	5′-GCTTGCCCAAGACACTGG-3′
Prop1-R	5′-CTTAGCCCTGCGGTTCTG-3′
Pou1f1-F	5′-CCACCAACGTGATGTCCAC-3′
Pou1f1-R	5′-GATGGCTGGTTTCCATAATGA-3′
Pomc-F	5′-TGGCCCTCCTGCTTCAGA-3′
Pomc-R	5′-GGATGCAAGCCAGCAGGTT-3′
Prl-F	5′-CCATGAACAGCCAAGTGTCA-3′
Prl-R	5′-TGGCAGAACAGAAGGTTTGA-3′
Tshb-F	5′-TTACCGAAGGGTATAAAATGAACAG-3′
Tshb-R	5′-GGAAAAGAGAACGACAGCATTC-3′
Fshb-F	5′-AAGTCGATCCAGCTTTGCAT-3′
Fshb-R	5′-TCCCTGGTGTAGCAGTAGCC-3′
Lhb-F	5′-CTGAGCCCAAGTGTGGTGT-3′
Lhb-R	5′-CACAGATGCTGGTGGTGAAG-3′
Gh-F	5′-CAAAGAGTTCGAGCGTGCCTA-3′
Gh-R	5′-TGGGATGGTCTCTGAGAAGCA-3′
β-Actin-F	5′-GTCGTACCACTGGCATTGTG-3′
β-Actin-R	5′-CTCTCAGCTGTGGTGGTGAA-3′

[a] F, forward; R, reverse.

solution (95% alcohol and 5% acetic acid) for 3 min, washed twice with 70% ethanol, and stained with H&E.

Statistical Analysis

Statistical analysis was performed using paired Student *t*-tests. Data are shown as mean ± SD. Statistical significance was set at $P < 0.05$.

RESULTS

Insertional Mutation by Bhr7 Transposon Creates Bbx-Null Rats

The Bhr7 transposon was previously described [4]. Briefly, it contains a splice acceptor IRES*rtTApA* cassette followed by the *Tyrosinase* gene. Insertion into an intron should truncate the endogenous transcript and result in pigmentation using an albino genetic background. Using the splinkerette PCR method [16], we identified one dark-pigmented male carrying the Bhr7 insertion at the 51 711 655 nucleotide position in intron 2 (51 708 413–51 712 818 nucleotides) of the *Bbx* gene (Fig. 1A) on chromosome 11 (http://www.ensembl.org/) [23]; this founder was referred to as $Bbx^{Tn/+}$. $Bbx^{Tn/+}$ F1 progeny were obtained by breeding the $Bbx^{Tn/+}$ founder with Wky female rats. Intercrosses of $Bbx^{Tn/+}$ F1 males and females generated F2 rats that underwent PCR-based gene-specific genotyping (Fig. 1B). From the genotype analysis of 202 F2 rats (33 litters) at Postnatal Days 7–10, the numbers of wild-type, $Bbx^{Tn/+}$, and $Bbx^{Tn/Tn}$ rats were 49 (24.3%), 127 (62.9%), and 26 (12.9%). The actual numbers of $Bbx^{Tn/Tn}$ rats were lower than expected, suggesting that some mutant rats died before genotyping. $Bbx^{Tn/Tn}$ rats had significantly smaller body sizes and weights compared with their littermates at 10 and 12 wk of age (Fig. 1, C and D). Next, we examined whether $Bbx^{Tn/Tn}$ rats were capable of producing progeny. Five $Bbx^{Tn/Tn}$ females mated with $Bbx^{Tn/+}$ males gave birth to a total of 35 pups. However, no $Bbx^{Tn/Tn}$ males (n = 5) mated with wild-type females yielded progeny, indicating that $Bbx^{Tn/Tn}$ males were infertile. To investigate the function of *Bbx* in rats, we examined *Bbx* expression patterns in various organs using real-time quantitative RT-PCR (RT-qPCR). We found that *Bbx* was highly expressed in the testes and moderately expressed in both male and female pituitary glands compared with other internal organs (Fig. 1E) and brain subregions (cortex, hippocampus, thalamus, and cerebellum; Supplemental Fig. S1; Supplemental Data are available online at www.biolreprod.org). In the testes and pituitary glands, *Bbx* expression levels were reduced by approximately 50% in heterozygous mutants and were undetectable in homozygous mutants (Fig. 1, F and G). These results suggest that Bhr7 insertion into the *Bbx* locus creates a null allele.

Bbx Appears Dispensable for the Expression of Many Pituitary Hormones

To detect *Bbx* expression in the pituitary gland, we performed immunohistochemistry using an antibody against BBX. We found that BBX localized in the nuclei of control pituitary glands, but was undetectable in *Bbx*-null mutants (Fig. 2A). Loss of BBX in the $Bbx^{Tn/Tn}$ pituitary was also confirmed by Western blotting (Fig. 2B). Using coimmunofluorescent staining of BBX and GH, we found that BBX was expressed in both GH-expressing and GH-nonexpressing cells (Fig. 2C). However, *Bbx* loss appeared to be dispensable for expression of *Prop1* and *Pou1f1* (Fig. 2D), both of which control pituitary organogenesis and direct hormonal gene expression [24]. Furthermore, we examined the expression of several hormonal genes, including *Gh1*, *Lhb*, *LSHb*, *Pomc*, *Prl*, and *Tshb*, using RT-qPCR in $Bbx^{+/+}$, $Bbx^{Tn/+}$, and $Bbx^{Tn/Tn}$ males (n = 3 per genotype) and females (n = 3 per genotype). We found no significant difference in the expression of these hormonal genes except for a reduction of *Lhb* expression in $Bbx^{Tn/Tn}$ females (Fig. 2E). Thus, most hormonal genes were unaffected in *Bbx*-null mutants.

Bbx Loss Impairs Spermiogenesis

Because BBX is highly expressed in the testes, we focused on potential testicular defects in *Bbx*-null rats. We dissected the male reproductive system and found that testes in $Bbx^{Tn/Tn}$ rats were smaller than those in their littermates ($Bbx^{+/+}$ and $Bbx^{Tn/+}$) at 12 wk of age (Fig. 3A). We measured testes weight normalized by body weight in $Bbx^{+/+}$, $Bbx^{Tn/+}$, and $Bbx^{Tn/Tn}$ rats at 3, 8, 10, 12, 15, and 20 wk of age. We observed a drastic decrease in the testes weight of $Bbx^{Tn/Tn}$ rats after 8 wk of age (Fig. 3B). Using immunohistochemistry, we found that BBX was highly expressed in developing spermatids in $Bbx^{+/+}$ testes, more specifically in round spermatids at stages V–VIII, elongated spermatids at stages IX–XI, and Sertoli cells (Supplemental Fig. S2). By contrast, BBX was undetectable in *Bbx*-null seminiferous tubules (Fig. 3C). Using Western blotting, we confirmed that BBX was expressed in $Bbx^{+/+}$ and $Bbx^{Tn/+}$ testes and absent in $Bbx^{Tn/Tn}$ mutant testes (Fig. 3D). We next examined the histology of *Bbx*-null and wild-type testes at 8, 10, and 20 wk of age. In wild-type testes, multiple cellular layers in seminiferous tubule cross-sections were revealed by H&E staining (Fig. 3E), and high-magnification views showed orderly arrangement of germ cells within the tubules (Fig. 3E). Similarly, normal appearance of seminiferous tubules was observed in 8-wk *Bbx*-null testes. However, the seminiferous tubules of $Bbx^{Tn/Tn}$ testes appeared to be abnormal, with clear atrophy after 10 wk of age (Fig. 3E). In high-magnification views, abnormal cells lacking the appearance of mature spermatozoa emerged at the lumens of the seminiferous tubules at 8 wk of age (Fig. 3E). From 10 wk of age onward, many tubules of the $Bbx^{Tn/Tn}$ testes showed germ cell loss and an increase in multinucleated giant cells (Fig. 3E). To further confirm that *Bbx* is expressed in round spermatids and Sertoli cells in the seminiferous epithelium, we performed coimmunofluores-

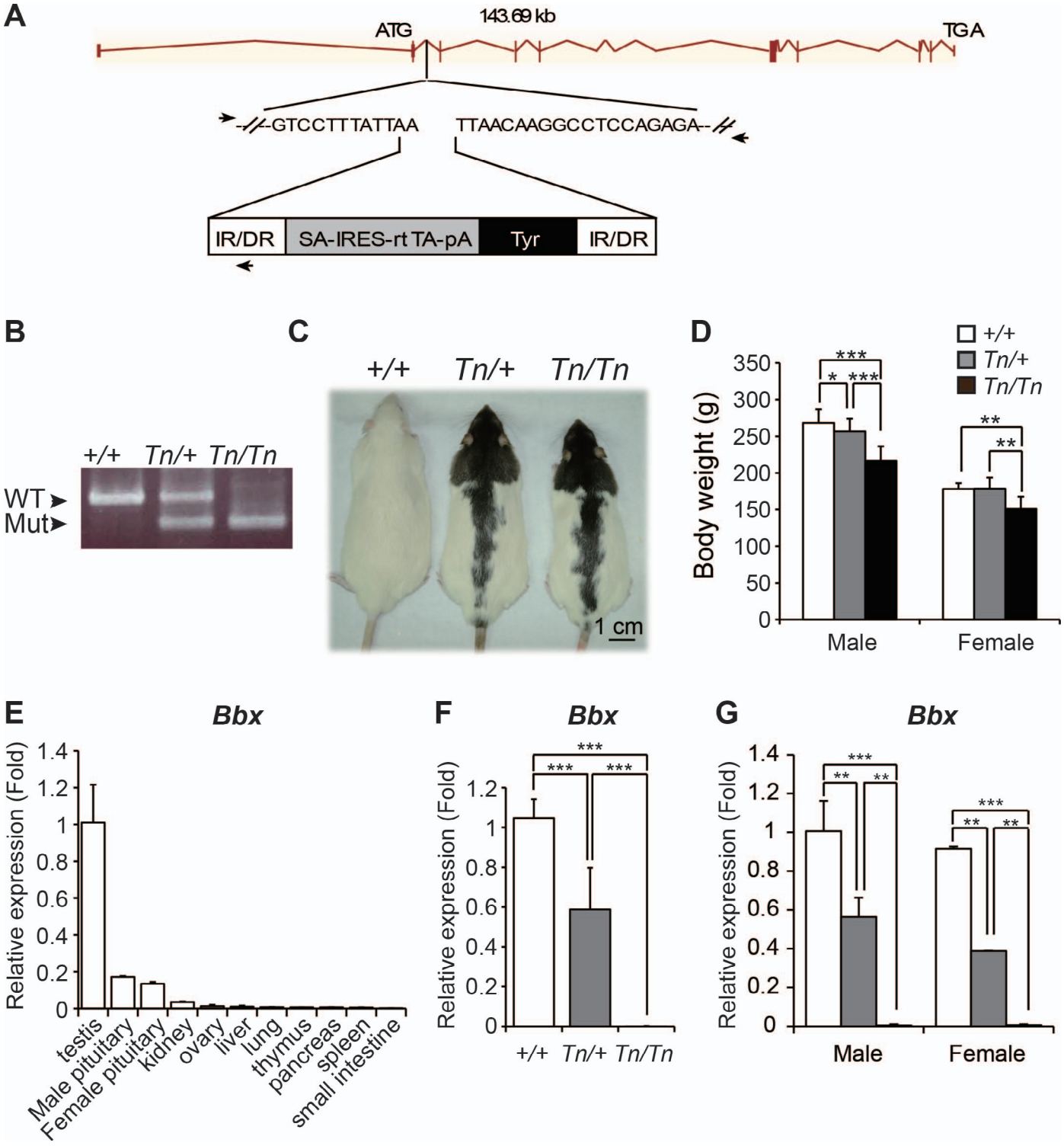

FIG. 1. Transposon insertion and expression of the *Bbx* locus in rats. **A**) Graphic illustration showing the Bhr7 transposon insertion into intron 2 of rat *Bbx*. **B**) Representative *Bbx*-specific genotyping by PCR. **C**) Representative image showing body size of wild-type, $Bbx^{Tn/+}$, and $Bbx^{Tn/Tn}$ rats at 12 wk of age. **D**) Body weight of wild-type (21 male and 6 female), $Bbx^{Tn/+}$ (22 male and 10 female), and $Bbx^{Tn/Tn}$ (15 male and 7 female) rats at 10 wk of age. **E**) RT-qPCR showed relative expression levels of *Bbx* in different organs of Wky male and female rats (n = 3) at 10 wk of age. **F**) RT-qPCR showed *Bbx* expression in the testes of wild-type (+/+), $Bbx^{Tn/+}$, and $Bbx^{Tn/Tn}$ rats (n = 3 per genotype) at 10 wk of age. **G**) RT-qPCR showed *Bbx* expression in the pituitary glands of wild-type (+/+), $Bbx^{Tn/+}$, and $Bbx^{Tn/Tn}$ male and female rats (n = 3 per genotype) at 10 wk of age. $^{*}P < 0.05$; $^{**}P < 0.01$; $^{***}P < 0.001$.

cence staining of antibodies against BBX and GATA4, which is expressed in postnatal mouse Sertoli cells [25]. We detected BBX in multiple layers of round spermatids and its coexpression with GATA4 in the nuclei of Sertoli cells in $Bbx^{+/+}$ seminiferous tubules (Fig. 3F). In $Bbx^{Tn/Tn}$ seminiferous tubules, Bbx was undetectable, whereas GATA4 was expressed in Sertoli cells (Fig. 3F). We further costained testes sections of 10-wk-old rats with antibodies against BBX and γH2AX, which marks DNA breaks during meiosis in spermatocytes [26, 27]. We found exclusive BBX staining in

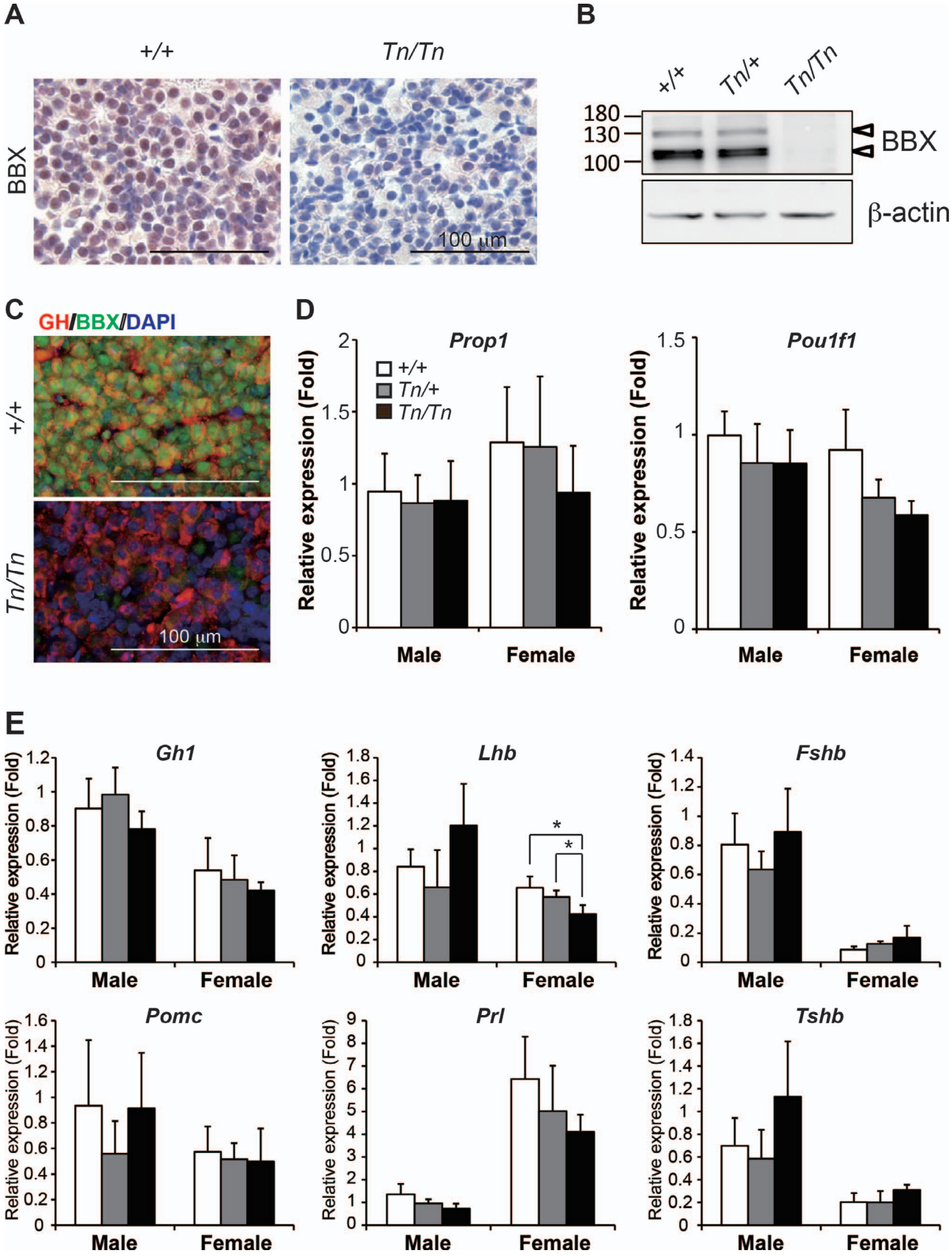

FIG. 2. Expression of *Bbx* and hormonal genes in pituitary glands of *Bbx* wild-type and mutant rats. **A**) Immunohistochemistry analysis showed the presence of nuclear BBX in the wild-type pituitary glands, but the lack of BBX in the $Bbx^{Tn/Tn}$ pituitary gland, at 10 wk of age. **B**) Western blot analysis showed the presence of BBX in wild-type and $Bbx^{Tn/+}$ pituitary glands, but the lack of BBX in the $Bbx^{Tn/Tn}$ pituitary gland. βActin served as an internal control. **C**) Coimmunofluorescent staining of BBX (green) and GH (red) showed the coexpression of BBX and GH in the wild-type pituitary gland, but the lack of BBX in the $Bbx^{Tn/Tn}$ pituitary gland. Nuclei were counterstained with DAPI. **D**) RT-qPCR showed relative levels of *Prop1* and *Pou1f1*, which encode

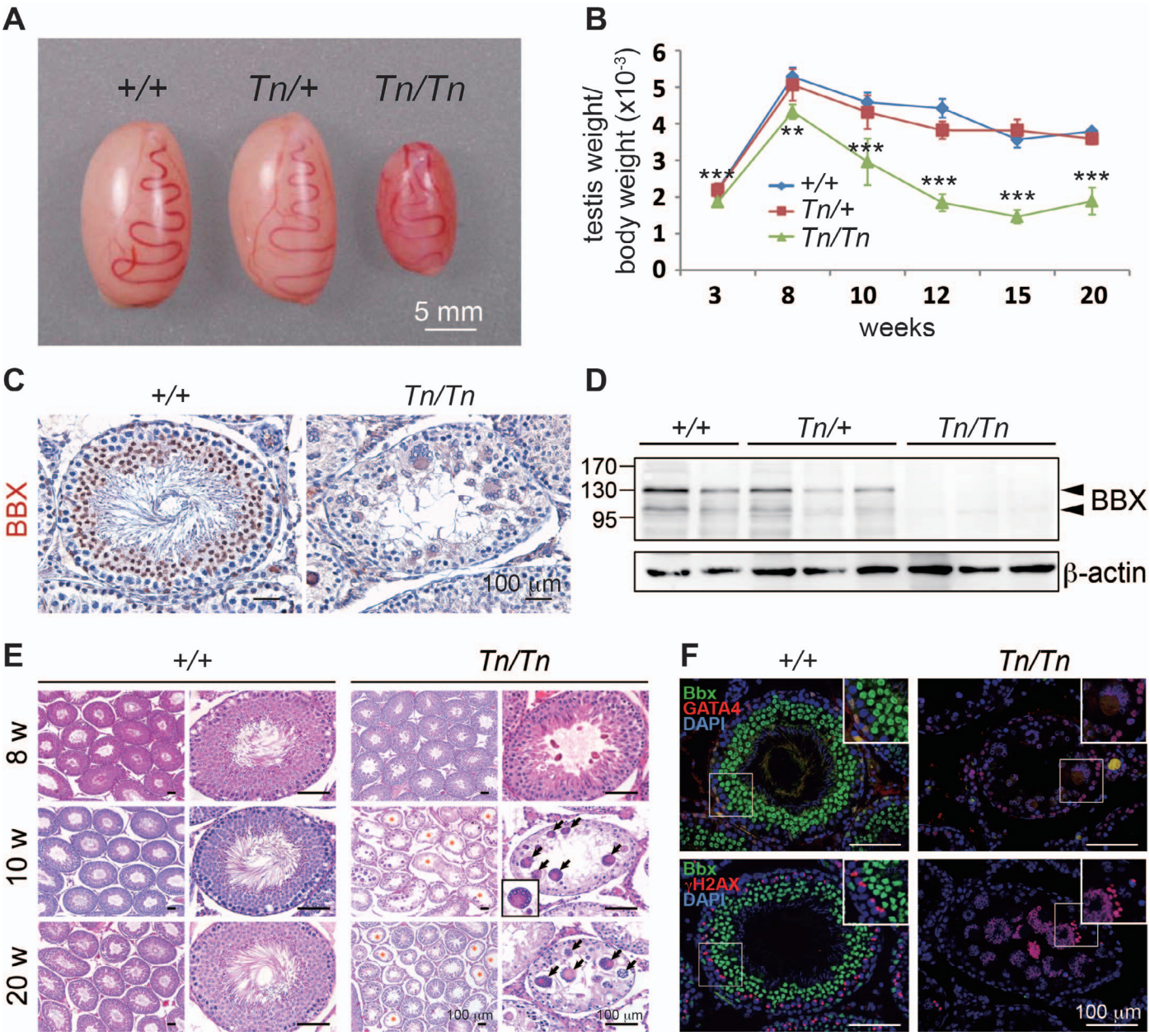

FIG. 3. Loss of *Bbx* causes testicular atrophy. **A**) Gross appearances of testes of wild-type (+/+), $Bbx^{Tn/+}$, and $Bbx^{Tn/Tn}$ rats at 12 wk of age. **B**) Quantification of testes weight normalized by body weight for wild-type (+/+), $Bbx^{Tn/+}$, and $Bbx^{Tn/Tn}$ rats at 3 wk (+/+, n = 3; Tn/+, n = 8; Tn/Tn, n = 6), 8 wk (+/+, n = 3; Tn/+, n = 9; Tn/Tn, n = 4), 10 wk (+/+, n = 9; Tn/+, n = 11; Tn/Tn, n = 5), 12 wk (+/+, n = 5; Tn/+, n = 8; Tn/Tn = 4), 15 wk (+/+, n = 3; Tn/+, n = 4; Tn/Tn, n = 3), and 20 wk (+/+, n = 4; Tn/+, n = 3; Tn/Tn, n = 3) of age. $^{**}P < 0.01$; $^{***}P < 0.001$. **C**) Immunohistochemical analysis of testes sections showed the presence of nuclear BBX in wild-type seminiferous tubules, but the lack of BBX in $Bbx^{Tn/Tn}$ seminiferous tubules at 10 wk of age. **D**) Western blot analysis showed the presence of BBX in wild-type (n = 2) and $Bbx^{Tn/+}$ (n = 3) testes, but not in $Bbx^{Tn/Tn}$ (n = 3) testes; βactin served as an internal control. **E**) H&E-stained sections of testes from wild-type and $Bbx^{Tn/Tn}$ rats at 8, 10, and 20 wk of age. Red asterisks indicate atrophic seminiferous tubules; black arrows indicate aberrant multinuclear giant cells. **F**) Coimmunofluorescent staining of BBX (green) and GATA4 (red; Sertoli cell marker) or γH2Ax (red; meiotic spermatocyte marker) shows BBX specifically in Sertoli cells and postmeiotic spermatids in the wild-type testis, but the lack of BBX in the $Bbx^{Tn/Tn}$ testis. Nuclei were counterstained by DAPI.

round spermatids, which were distinct from γH2AX-positive spermatocytes (Fig. 3F). In $Bbx^{Tn/Tn}$ testes, γH2AX-stained cells were disorganized and detached in the lumens of atrophic tubules (Fig. 3F). Taken together, these results suggest that *Bbx* is expressed in Sertoli cells and postmeiotic spermatids in the seminiferous tubules, indicative of its role in spermiogenesis.

transcription factors for pituitary organogenesis and hormonal gene expression, in the pituitary glands of wild-type (+/+), $Bbx^{Tn/+}$, and $Bbx^{Tn/Tn}$ males (n = 3 per genotype) and females (n = 3 per genotype) at 10 wk of age. **E**) RT-qPCR showed relative expression levels of *GH1*, *Lhb* (luteinizing hormone subunit β), *Fshb* (follicle-stimulating hormone subunit β), *Pomc* (pro-opiomelanocortin), *Prl* (prolactin), and *Tshb* (thyroid-stimulating hormone subunit β). $^{*}P < 0.05$.

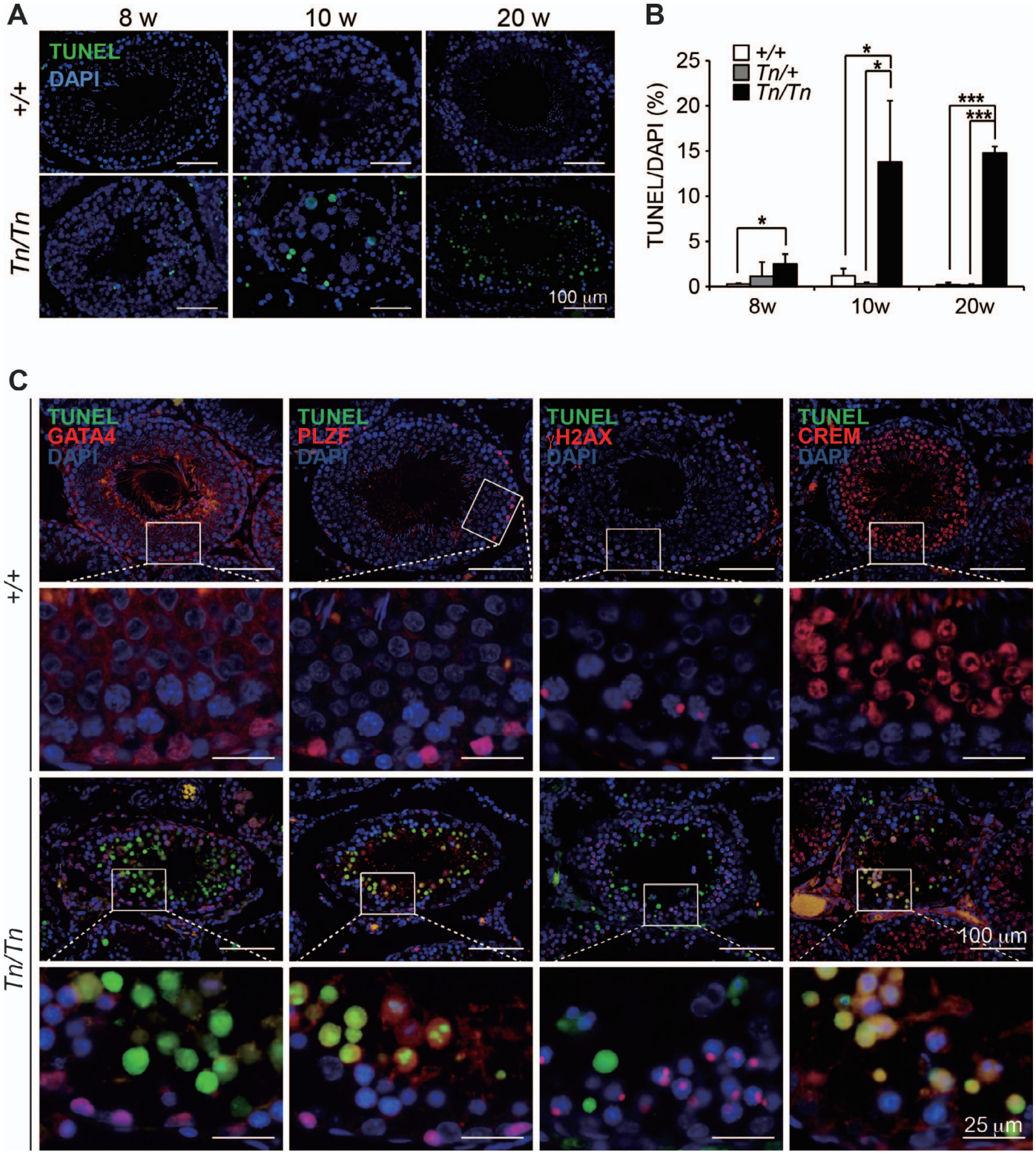

FIG. 4. Increased TUNEL-positive spermatids in $Bbx^{Tn/Tn}$ testes. **A**) $Bbx^{Tn/Tn}$ seminiferous tubules exhibited more TUNEL-positive cells (green) than wild-type seminiferous tubules at 8, 10, and 20 wk of age. **B**) Quantification of TUNEL-positive cells in wild-type, $Bbx^{Tn/+}$, and $Bbx^{Tn/Tn}$ seminiferous tubules at 8 wk (n = 3 per genotype), 10 wk (+/+, n = 4; Tn/+, n = 3; Tn/Tn, n = 4), and 20 wk (n = 3 per genotype) of age. *$P < 0.05$; ***$P < 0.001$. **C**) Low-magnification (upper panels) and high-magnification (lower panels; boxed areas of corresponding upper images) views of coimmunofluorescent staining of TUNEL (green) and GATA4 (red; Sertoli cell marker), PLZF (red; spermatogonial cell marker), γH2Ax (red; meiotic spermatocyte marker), or CREM (red; postmeiotic spermatid marker) showed greater coexpression of TUNEL and CREM1-positive signals in the seminiferous tubules of $Bbx^{Tn/Tn}$ rats than those of wild-type rats at 10 wk of age. Nuclei were counterstained by DAPI.

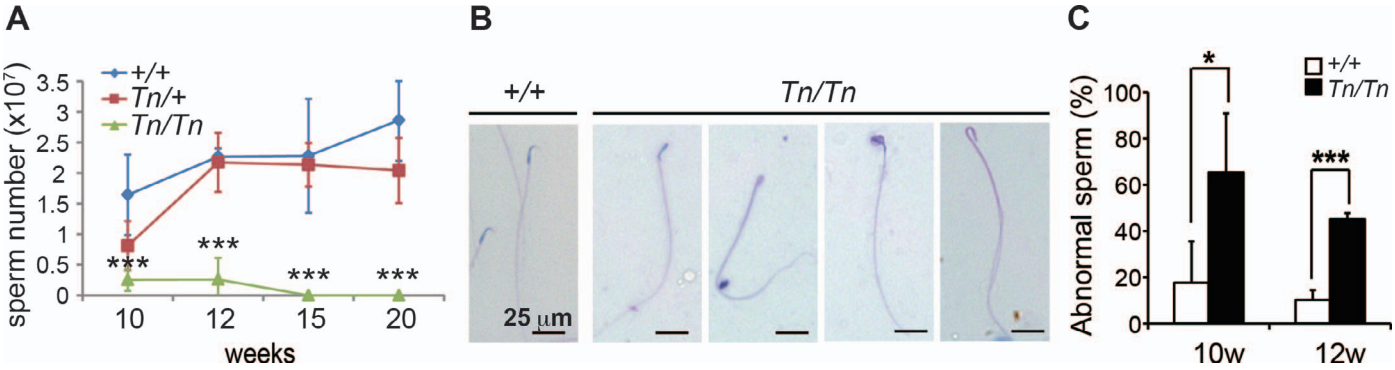

FIG. 5. Impaired sperm production in $Bbx^{Tn/Tn}$ rats. **A**) Number of sperm in the epididymis of wild-type (+/+), $Bbx^{Tn/+}$, and $Bbx^{Tn/Tn}$ rats at 10 wk (+/+, n = 8; Tn/+, n = 8; Tn/Tn, n = 5), 12 wk (+/+, n = 4; Tn/+, n = 6; Tn/Tn, n = 10), 15 wk (+/+, n = 3; Tn/+, n = 4; Tn/Tn, n = 3), and 20 wk (n = 3 per genotype) of age. **B**) Images of abnormal sperm morphology in $Bbx^{Tn/Tn}$ rats compared with wild-type rats at 12 wk of age. **C**) Quantification of abnormal sperm in the epididymis of wild-type (+/+) and $Bbx^{Tn/Tn}$ rats at 10 and 12 wk of age (n = 3 per genotype and time point). $^*P < 0.05$; $^{***}P < 0.001$.

Increased TUNEL-Positive Cells in Bbx*-Deficient Seminiferous Tubules*

We further examined whether apoptosis might cause germ cell loss in *Bbx*-null mutant rats. $Bbx^{Tn/Tn}$ seminiferous tubules exhibited more TUNEL-positive cells at 8 wk of age and even more cells at 10 and 20 wk of age compared with wild-type seminiferous tubules, which showed undetectable TUNEL staining or only a few TUNEL-positive cells (Fig. 4A). When we quantified TUNEL-positive cells in the seminiferous tubules of $Bbx^{+/+}$, $Bbx^{Tn/+}$, and $Bbx^{Tn/Tn}$ rats at 8, 10, 12, and 20 wk of age, we found a significantly greater number of TUNEL-positive cells in $Bbx^{Tn/Tn}$ seminiferous tubules than in wild-type or $Bbx^{Tn/+}$ tubules at all time points (Fig. 4B). We further examined whether $Bbx^{Tn/Tn}$ Sertoli cells also underwent apoptosis. Immunofluorescent staining revealed that GATA4-positive cells were TUNEL-negative cells (Fig. 4C), suggesting that $Bbx^{Tn/Tn}$ Sertoli cells are apoptosis-resistant cells. Moreover, we performed TUNEL assay and immunofluorescent staining of PLZF [28] for marking spermatogonia, γH2AX for marking spermatocytes [26, 27], and CREM for marking postmeiotic spermatids [29, 30]. We found that TUNEL-positive signals mainly overlapped with CREM-positive spermatids, but not with GATA4-, PLZF-, or γH2AX-positive cells (Fig. 4C). These findings suggest that loss of *Bbx* causes death of postmeiotic spermatids and impairs spermiogenesis.

Impaired Sperm Production and Motility in Bbx*-Null Rats*

By counting sperm number in the epididymis of wild-type, $Bbx^{Tn/+}$, and $Bbx^{Tn/Tn}$ rats, we found a drastic reduction of sperm number in $Bbx^{Tn/Tn}$ rats compared with wild-type or $Bbx^{Tn/+}$ rats at 10 and 12 wk of age (Fig. 5A). After 15 wk of age, $Bbx^{Tn/Tn}$ rats exhibited azoospermia, whereas $Bbx^{Tn/+}$ and wild-type rats had substantial amounts of spermatozoa (Fig. 5A). At 10 wk of age, spermatozoa were detected in the epididymis of $Bbx^{Tn/Tn}$ rats, but were largely abnormal, with misshapen sperm heads in contrast to the hook-shaped heads of wild-type sperm (Fig. 5B). The amount of abnormal spermatozoa produced in $Bbx^{Tn/Tn}$ rats was significantly higher than that produced in wild-type rats (Fig. 5C). In addition, we observed that the spermatozoa produced in $Bbx^{Tn/Tn}$ rats were immotile (Supplemental Movies S1 and S2). Taken together, our results demonstrate that the infertility of $Bbx^{Tn/Tn}$ rats was mainly caused by impaired spermiogenesis.

DISCUSSION

In this study, we used PB-based mutagenesis screening [4] to identify *Bbx*-null rats, which were smaller than wild-type rats and exhibited male infertility. Two major organs, the pituitary gland and testes, were specifically analyzed due to their higher *Bbx* expression compared with other organs in wild-type Wky rats. Loss of *Bbx* in the pituitary glands appeared to be dispensable for pituitary organogenesis and hormonal gene expression. Although previous studies [12, 14] suggested that *Bbx* has a role in cortex and hippocampus, we did not observe obvious behavioral phenotypes in $Bbx^{Tn/Tn}$ rats compared to controls (data not shown). In the testes, *Bbx* was expressed in the Sertoli cells and postmeiotic round spermatids. By 8 wk of age, histology of the testes appeared to be normal in $Bbx^{Tn/Tn}$ rats, suggesting that *Bbx* is dispensable for the early spermatogenesis. After 10 wk of age, loss of *Bbx* resulted in the presence of aberrant multinucleated giant cells and apoptotic spermatids in the seminiferous tubules. These defects might be caused by *Bbx* deficiency in either the Sertoli cells or round spermatids, or both cell types, at the adult stage. Subsequently, loss of *Bbx* caused azoospermia and infertility. Aberrant multinucleated giant cells were previously observed in rats with vasectomy-induced spermatogenic impairments [31]. In addition, genetically modified mice, such as *Crem*- [29, 30], *Trf2*- [32], and *Fdnc3a*-deficient mice [33], display spermatogenic defects with aberrant multinucleated giant cells in the seminiferous tubules.

A recent public phenotyping screen (the Wellcome Trust Sanger Institute Mouse Portal; http://www.sanger.ac.uk/mouseportal/) [34], which identified $Bbx^{tm1a\ (EUCOMM)Wtsi}$ knockout mice carrying a splicing acceptor reporter-tagged insertion in intron 5 of the *Bbx* locus, revealed decreased lean mass in homozygous males and females; decreased body length, heart weight, and bone mineral density/content in homozygous females; and abnormal tooth morphology in homozygous mutant males. However, the reproductive ability of *Bbx* mutant mice appeared to be unaffected. As previously described, the complete spermatogenic process varies among species [5, 7], which could lead to different outcomes of the loss of *Bbx* between mice and rats. It is also possible that the insertion into intron 5 in the mouse does not create a null allele. Thus, genetically altered rats could serve as alternative animal models for better understanding of comparative gene function across different species.

In summary, our findings demonstrate the fundamental role of BBX in spermiogenesis in rats using transposon-mediated

insertional mutagenesis. Our study provides an entry for future studies of the BBX transcription factor and its potential target genes for regulating spermiogenesis. In addition, future clinical studies could examine whether BBX is associated with azoospermia in humans.

ACKNOWLEDGMENT

The authors thank Dr. Li-Ru You for comments on this manuscript, as well as Yi-Hsuan Chiang and Ying-Ling Sun for their initial assistance.

REFERENCES

1. Kitada K, Ishishita S, Tosaka K, Takahashi R, Ueda M, Keng VW, Horie K, Takeda J. Transposon-tagged mutagenesis in the rat. Nat Methods 2007; 4:131–133.
2. Kitada K, Keng VW, Takeda J, Horie K. Generating mutant rats using the Sleeping Beauty transposon system. Methods 2009; 49:236–242.
3. Lu B, Geurts AM, Poirier C, Petit DC, Harrison W, Overbeek PA, Bishop CE. Generation of rat mutants using a coat color-tagged Sleeping Beauty transposon system. Mamm Genome 2007; 18:338–346.
4. Furushima K, Jang CW, Chen DW, Xiao N, Overbeek PA, Behringer RR. Insertional mutagenesis by a hybrid piggyBac and sleeping beauty transposon in the rat. Genetics 2012; 192:1235–1248.
5. Hermo L, Pelletier RM, Cyr DG, Smith CE. Surfing the wave, cycle, life history, and genes/proteins expressed by testicular germ cells. Part 1: background to spermatogenesis, spermatogonia, and spermatocytes. Microsc Res Tech 2010; 73:241–278.
6. Hogarth CA, Griswold MD. The key role of vitamin A in spermatogenesis. J Clin Invest 2010; 120:956–962.
7. Clermont Y. Kinetics of spermatogenesis in mammals: seminiferous epithelium cycle and spermatogonial renewal. Physiol Rev 1972; 52: 198–236.
8. Leblond CP, Clermont Y. Definition of the stages of the cycle of the seminiferous epithelium in the rat. Ann N Y Acad Sci 1952; 55:548–573.
9. Oakberg EF. Duration of spermatogenesis in the mouse and timing of stages of the cycle of the seminiferous epithelium. Am J Anat 1956; 99: 507–516.
10. Heller CG, Clermont Y. Spermatogenesis in man: an estimate of its duration. Science 1963; 140:184–186.
11. Clermont Y. The cycle of the seminiferous epithelium in man. Am J Anat 1963; 112:35–51.
12. Chen T, Zhou L, Yuan Y, Fang Y, Guo Y, Huang H, Zhou Q, Lv X. Characterization of Bbx, a member of a novel subfamily of the HMG-box superfamily together with Cic. Dev Genes Evol 2014; 224:261–268.
13. Sanchez-Diaz A, Blanco MA, Jones N, Moreno S. HBP2: a new mammalian protein that complements the fission yeast MBF transcription complex. Curr Genet 2001; 40:110–118.
14. Dixon C, Harvey T, Smith A, Gronostajski R, Bailey T, Piper M. Nuclear factor one X regulates Bobby Sox during development of the mouse forebrain. Cell Mol Neurobiol 2013; 33:867–873.
15. Choi YA, Seol MY, Shin HI, Park EK. Bobby Sox homology regulates odontoblast differentiation of human dental pulp stem cells/progenitors. Cell Commun Signal 2014; 12:35.
16. Potter CJ, Luo L. Splinkerette PCR for mapping transposable elements in *Drosophila*. PLoS One 2010; 5:e10168.
17. Latendresse JR, Warbrittion AR, Jonassen H, Creasy DM. Fixation of testes and eyes using a modified Davidson's fluid: comparison with Bouin's fluid and conventional Davidson's fluid. Toxicol Pathol 2002; 30: 524–533.
18. Lu T-L, Chang J-L, Liang C-C, You L-R, Chen C-M. Tumor spectrum, tumor latency and tumor incidence of the Pten-deficient mice. PLoS One 2007; 2:e1237.
19. Lu T-L, Huang Y-F, You L-R, Chao N-C, Su F-Y, Chang J-L, Chen C-M. Conditionally ablated Pten in prostate basal cells promotes basal-to-luminal differentiation and causes invasive prostate cancer in mice. Am J Pathol 2013; 182:975–991.
20. Yu Y-R, You L-R, Yan Y-T, Chen C-M. Role of OVCA1/DPH1 in craniofacial abnormalities of Miller-Dieker syndrome. Hum Mol Genet 2014; 23:5579–5596.
21. Liang C-C, Lu T-L, Yu Y-R, You L-R, Chen C-M. β-catenin activation drives thymoma initiation and progression in mice. Oncotarget 2015; 6: 13978–13993.
22. Lu T-L, Chen C-M. Differential requirements for β-catenin in murine prostate cancer originating from basal versus luminal cells. J Pathol 2015; 236:290–301.
23. Flicek P, Amode MR, Barrell D, Beal K, Billis K, Brent S, Carvalho-Silva D, Clapham P, Coates G, Fitzgerald S, Gil L, Girón CG, et al. Ensembl 2014. Nucleic Acids Res 2014; 42:D749–D755.
24. Mortensen AH, MacDonald JW, Ghosh D, Camper SA. Candidate genes for panhypopituitarism identified by gene expression profiling. Physiol Genomics 2011; 43:1105–1116.
25. Imai T, Kawai Y, Tadokoro Y, Yamamoto M, Nishimune Y, Yomogida K. In vivo and in vitro constant expression of GATA-4 in mouse postnatal Sertoli cells. Mol Cell Endocrinol 2004; 214:107–115.
26. Mahadevaiah SK, Turner JM, Baudat F, Rogakou EP, de Boer P, Blanco-Rodriguez J, Jasin M, Keeney S, Bonner WM, Burgoyne PS. Recombinational DNA double-strand breaks in mice precede synapsis. Nat Genet 2001; 27:271–276.
27. Hamer G, Roepers-Gajadien HL, van Duyn-Goedhart A, Gademan IS, Kal HB, van Buul PP, de Rooij DG. DNA double-strand breaks and gamma-H2AX signaling in the testis. Biol Reprod 2003; 68:628–634.
28. Costoya JA, Hobbs RM, Barna M, Cattoretti G, Manova K, Sukhwani M, Orwig KE, Wolgemuth DJ, Pandolfi PP. Essential role of Plzf in maintenance of spermatogonial stem cells. Nat Genet 2004; 36:653–659.
29. Nantel F, Monaco L, Foulkes NS, Masquilier D, LeMeur M, Henriksen K, Dierich A, Parvinen M, Sassone-Corsi P. Spermiogenesis deficiency and germ-cell apoptosis in CREM-mutant mice. Nature 1996; 380:159–162.
30. Blendy JA, Kaestner KH, Weinbauer GF, Nieschlag E, Schutz G. Severe impairment of spermatogenesis in mice lacking the CREM gene. Nature 1996; 380:162–165.
31. Ren L, Weng Q, Kishimoto M, Watanabe G, Jaroenporn S, Taya K. Effect of short period vasectomy on FSH, LH, inhibin and testosterone secretions, and sperm motility in adult male rats. Exp Anim 2011; 60: 47–56.
32. Zhang D, Penttila TL, Morris PL, Teichmann M, Roeder RG. Spermiogenesis deficiency in mice lacking the Trf2 gene. Science 2001; 292:1153–1155.
33. Obholz KL, Akopyan A, Waymire KG, MacGregor GR. FNDC3A is required for adhesion between spermatids and Sertoli cells. Dev Biol 2006; 298:498–513.
34. van der Weyden L, White J, Adams D, Logan D. The mouse genetics toolkit: revealing function and mechanism. Genome Biol 2011; 12:224.